frontiers | Frontiers in Astronomy and Space Sciences

TYPE Original Research
PUBLISHED 11 November 2024
DOI 10.3389/fspas.2024.1489982

OPEN ACCESS

EDITED BY
Ryszard Szczerba,
Polish Academy of Sciences, Poland

REVIEWED BY
Franco Cataldo,
Actinium Chemical Research Institute, Italy
Ransel Barzaga,
Spanish National Research Council (CSIC), Spain

*CORRESPONDENCE
Yong Zhang,
zhangyong5@mail.sysu.edu.cn

RECEIVED 02 September 2024
ACCEPTED 25 September 2024
PUBLISHED 11 November 2024

CITATION
Liao X-X, Zhang Y and Sadjadi S (2024) Exploring the possibility of polycyclic aromatic hydrocarbons and fulleranes as the carrier of the 21 micron emission feature. *Front. Astron. Space Sci.* 11:1489982. doi: 10.3389/fspas.2024.1489982

Exploring the possibility of polycyclic aromatic hydrocarbons and fulleranes as the carrier of the 21 micron emission feature

Xuan-Xiang Liao[1], Yong Zhang[1,2]* and SeyedAbdolreza Sadjadi[2]

[1]School of Physics and Astronomy, Sun Yat-sen University, Zhuhai, Guangdong, China, [2]The Laboratory for Space Research, Faculty of Science, The University of Hong Kong, Hong KongSAR, China

Introduction: The 21 μm emission feature discovered in a small sample of carbon-rich protoplanetary nebulae has remained unidentified for over 30 years. A dozen of different molecular species (both organics and inorganics) have been proposed as the carrier candidates of this important feature, among which polycyclic aromatic hydrocarbons (PAHs) and fulleranes (hydrogenated fullerenes) have yet to be sufficiently examined.

Method: In this study, we attempt to fit the 21 μm features in observed spectra of the above-mentioned astronomical sources via theoretically simulated spectra of various PAHs and fulleranes, aiming to investigate whether the two hydrocarbon families can reproduce the 21 μm feature.

Results and Discussion: Based on the fitting outcomes we conclude that fulleranes can provide a more plausible explanation for the origin of 21 μm feature than PAHs.

KEYWORDS

infrared, polycyclic aromatic hydrocarbons, fullerenes, fulleranes, protoplanetary nebulae, astrochemistry

1 Introduction

As a low- or intermediate-mass star progresses into the final stage of the asymptotic giant branch (AGB), its circumstellar envelope is detached from the stellar surface, and the effective temperature rises (e.g., Kwok, 1993; 2024). When the center star is sufficiently hot, the envelope is ionized, initiating the formation of a planetary nebula (PN). During the transition from the AGB to PN phases, there is a brief evolutionary phase (~10^3 yr), called protoplanetary nebula (PPN, see, e.g., Volk Kwok, 1989). Observing PPNe is challenging because their main radiation bands are in the infrared wavelength region and almost without emission lines in the optical region. Infrared instruments such as the Infrared Astronomical Satellite (*IRAS*, Neugebauer et al., 1984), the Infrared Space Observatory (*ISO*, Van Winckel, 2003), and the *Spitzer* Space Telescope (Gehrz et al., 2007) have significantly enhanced our ability to observe and study PPNe.

Despite evolving from an AGB star's envelope, a PPN's infrared spectrum exhibits substantial variations with the appearance of a group of Unidentified Infrared Emission

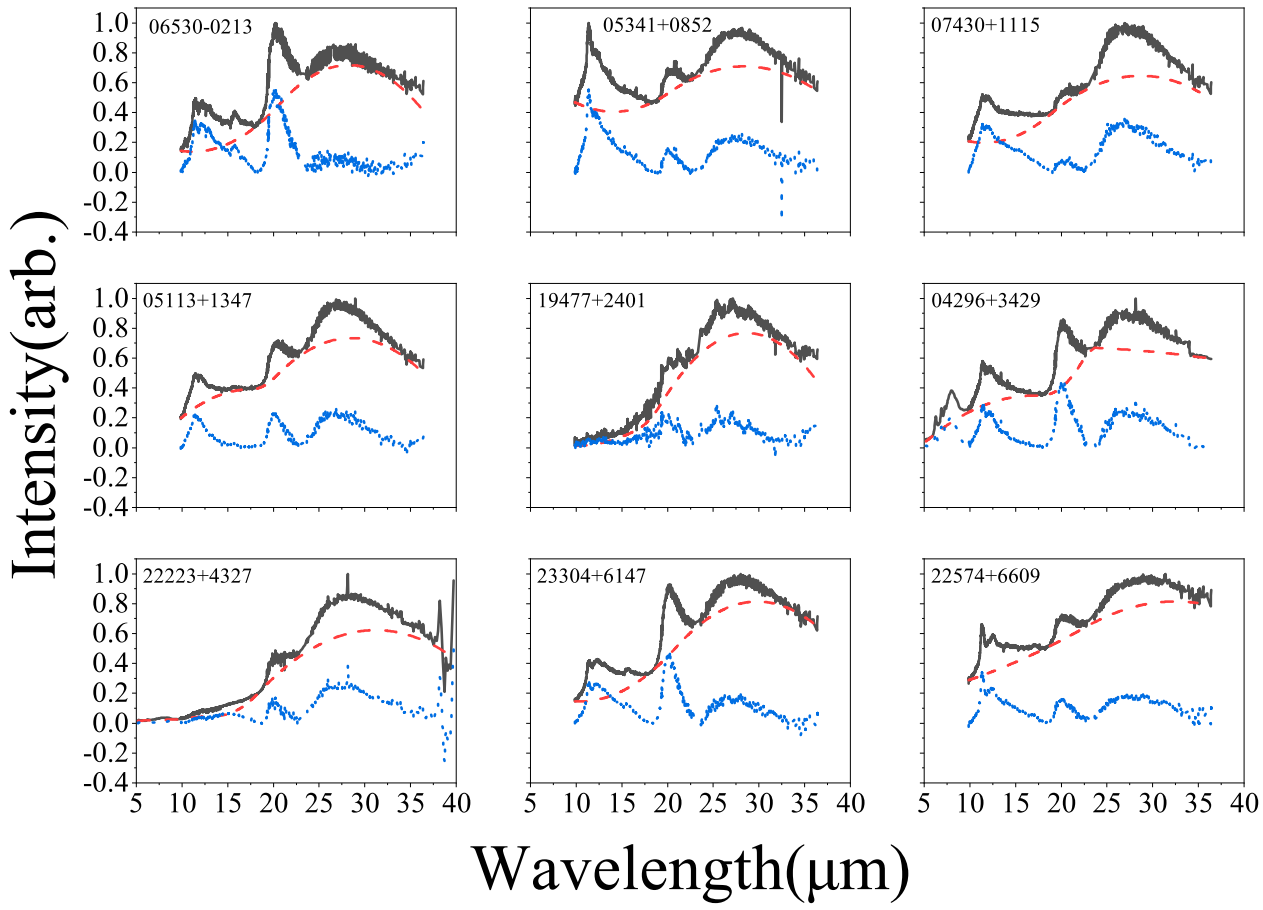

FIGURE 1
Normalized *Spitzer* spectra of the 21 μm sources (solid curves). The continua (red dashed curves) are subtracted to obtain the spectra for fitting (blue dotted curves).

(UIE) bands at 3.3, 3.4, 6.2, 6.9, 7.7, 8.6, 11.3, and 12.7 μm (Duley and Williams, 1981; Buss Jr et al., 1990). suggesting the formation of complex hydrocarbons with aromatic and aliphatic functional groups during the PPN stage (Kwok, 2004). The chemical processes that lead to the production of these organic molecules in PPN have yet to be uncovered.

In addition, an UIE feature at 21 μm was first discovered by Kwok et al. (1989) in four carbon-rich PPNe from the *IRAS* database. Over the subsequent three decades, researchers have detected a total of 31 sources exhibiting this feature from the *IRAS*, *ISO*, and *Spitzer* Space Telescope databases (García-Lario et al., 1999; Hrivnak et al., 2000; 2009; Cerrigone et al., 2011; Volk et al., 2011; Matsuura et al., 2014; Gładkowski et al., 2019). Among them, 20 are within the Milky Way galaxy, nine are within the Large Magellanic Cloud (LMC), and two are within the Small Magellanic Cloud (SMC). The 21 μm emission feature has an asymmetric profile that expands over the wavelength range of 17.4–23.4 μm with a maximum flux centered around 20.1 μm. The feature is characterized by a rapid rise in the short and gradually declining at the long wavelength side (Volk et al., 2020). The 21 μm feature is mostly accompanied by a broad emission at 30 μm and a plateau emission at 11–17 μm. The exclusive presence of the 21 μm feature in PPNe may hold a vital clue in understanding PPN chemistry. However, the identification of its carrier remains highly controversial. So far different carrier candidates have been proposed (see, Volk et al., 2020, for a list). Considering that the carrier must meet two criteria: 1) the involved elements must be abundant enough to account for the intense 21 μm emission; 2) other emission bands produced by the substance must resemble the observed spectrum, Zhang et al. (2009) examined nine Si-, Fe-, and Ti-bearing carrier candidates, and found that most of them except FeO nanoparticles do not satisfy the two criteria. Subsequently, Li et al. (2013) found evidence that FeO cannot be responsible for the 21 μm feature.

Apart from inorganic compounds, complex organic molecules such as polycyclic aromatic hydrocarbons (PAHs) and hydrogenated fullerenes (fulleranes), could also emit at around 21 μm. Distinguishing from a single inorganic species, PAHs and fulleranes are presenting hydrocarbon families with specific molecular structures. PAHs contain a large cyclic conjugate structure, allowing them to be stable in interstellar space, and are being considered as possible carriers of some groups of UIEs (3.3, 6.2, 7.7, 8.6, 11.3, and 12.7 μm) (Tielens, 2008; Duley and Williams, 1981). Papoular (2011) found that PAH-like molecules can reproduce the 21 μm feature. Fullerene (C_{60}) was first discovered in the PN Tc1 (Cami et al., 2010) and subsequently observed in different circumstellar environments including the PPN (García-Hernández et al., 2010; 2011a; b;

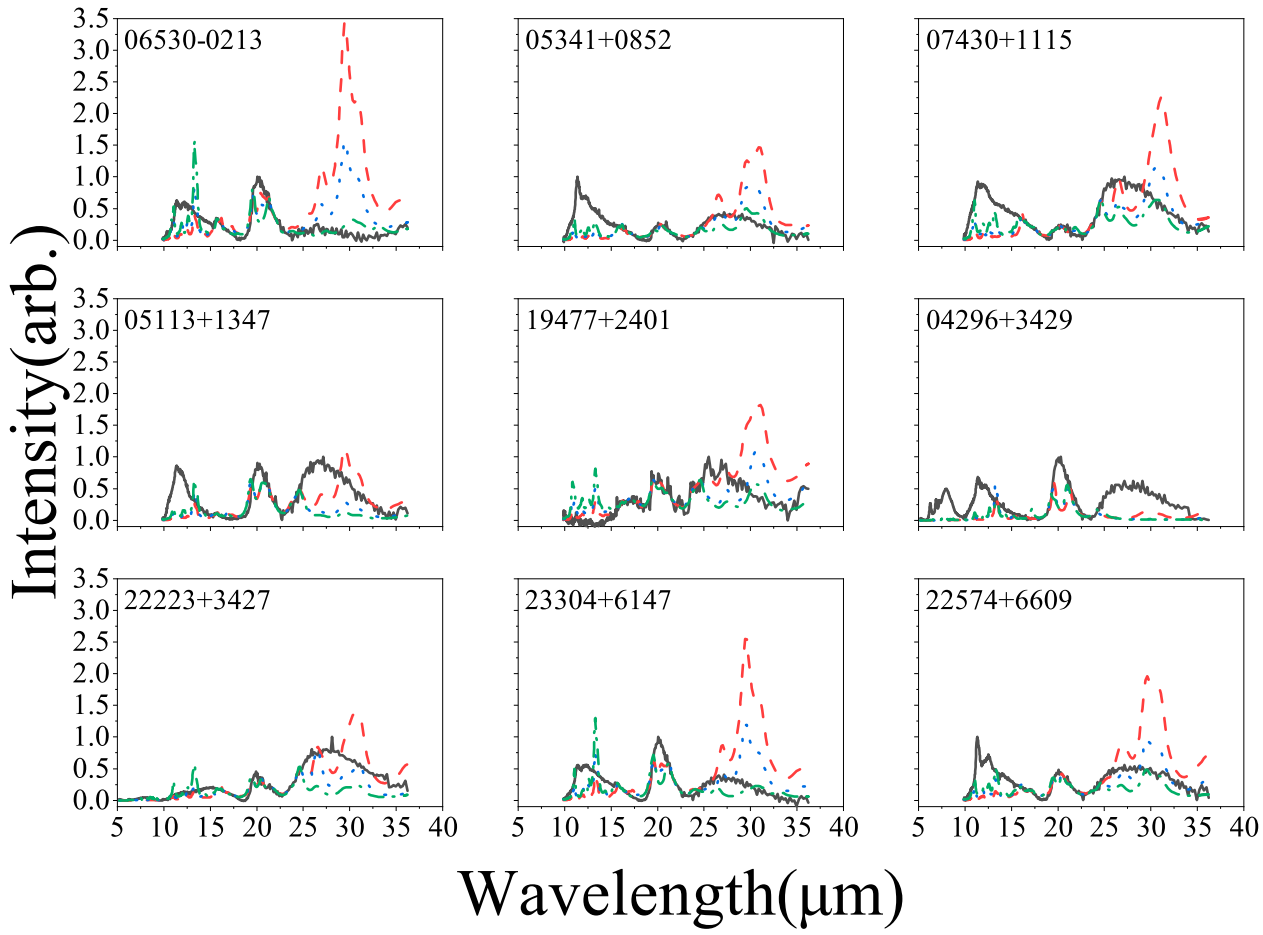

FIGURE 2
Fitting the observed spectra (solid curves) using the theoretical spectra of PAHs at 100 K (red dashed curves), 125 K (green dotted curves), and 150 K (blue dashed-dotted curves).

Sellgren et al., 2010; Gielen et al., 2011; Zhang and Kwok, 2011; Evans et al., 2012; Roberts et al., 2012; Otsuka et al., 2013). In laboratory conditions, C_{60} can be quickly hydrogenated into $C_{60}H_{36}$ by atomic hydrogen (Cataldo and Iglesias-Groth, 2009) and would undergo rapid dehydrogenation when heated to around 550 *K* (Rüchardt et al., 1993). So far there is no compelling evidence for the presence of circumstellar fulleranes, although tentative detection has been anticipated (Zhang et al., 2017; Palotás et al., 2020). Fullerene cage structure maintains in harsh astronomical environments (Sadjadi and Parker, 2021) to form fulleranes and emit UIEs. The possibility of fulleranes as the carrier of the 21 μm feature was raised by Webster (1995) and revisited by Zhang et al. (2020).

In comparison to other astrochemically relevant species, PAHs and fulleranes have certain advantages to account for the 21 μm emission. The cosmic abundances of carbon and hydrogen are high. The 21 μm features are revealed only in carbon-rich sources, suggesting its carrier is more likely to be carbon-bearing. Moreover, considering the different sizes, structures, charge states, and impurities, the numbers of PAHs and fulleranes could be large, providing a very flexible way to fit the observed spectrum. However, their likehoods as the 21 μm feature carrier have not been sufficiently evaluated. To this end, we perform spectral fittings of the observations utilizing the theoretical spectra of PAHs and fulleranes, aiming to investigate how well the two hydrocarbon families reproduce the 21 μm feature.

The paper is structured as follows: Section 2 presents the methodology and the data used. In Section 3 we discuss the goodness of different materials as the carrier of the 21μm emission feature. Section 4 presents our conclusions.

2 Methodology

2.1 Observational spectra

The *Spitzer Space Telescope* observed 11 sources exhibiting the 21 μm emission feature between 2004 and 2008 as part of the programs No. 20208 (PI: B. Hrivnak) and 93 (PI: D. Cruikshank), including IRAS 04296 + 3,429, IRAS 05113 + 1,347, IRAS 05341 + 0,852, IRAS 06530-0,213, IRAS 07134 + 1,005, IRAS 07430 + 1,115, IRAS 19477 + 2,401, IRAS 20000 + 3,239, IRAS 22223 + 4,327, IRAS 22574 + 6,609, and IRAS 23304 + 6,147. Among them, IRAS 07134 + 1,005 and IRAS 20000 + 3,239 exhibit exceptionally strong 21

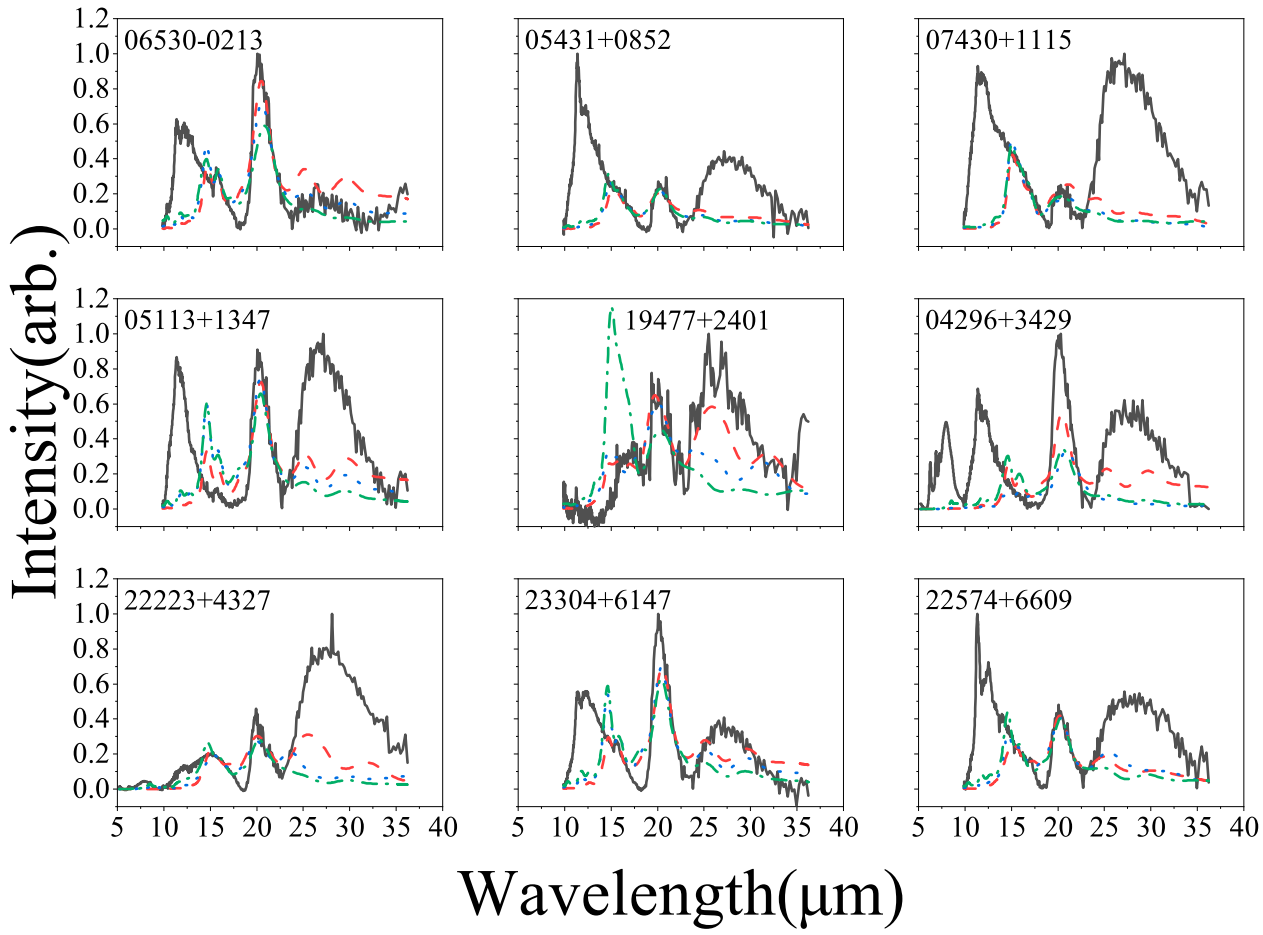

FIGURE 3
Same as Figure 2 but for fulleranes.

μm emissions, which are saturated in the observations. The *Spitzer* spectra of the other nine PPNe were extracted from the *Spitzer* archive for our analysis (see Zhang et al., 2010, for the details of the spectra and the data processing), covering a wavelength range from 9.9 to 37.2 μm. IRAS 04296 + 3,429 and IRAS 22223 + 4,327 were also observed using the short-low (SL) module in programs 30036 (PI: G. Fazio) and 45 (PI: T. Roellig), thus their spectra have a larger wavelength coverage (5.5–37.2 μm.)

To subtract the continuum underlying the features, we selected the concave points in the spectra as anchors. A spline interpolation was utilized to construct a curve that passes through all selected anchors. Then constructed curve was subtracted from the observed spectrum for the subsequent fitting. The continuum-subtracted spectra are shown in Figure 1.

2.2 Theoretical spectra of PAHs

Theoretical Infrared (IR) spectra of PAH molecules calculated at density functional theory (DFT) (Parr, 1985; Mattioda et al., 2020) were obtained from the NASA Ames PAH IR Spectroscopic Database[1] (PAHdb Bauschlicher et al., 2010; 2018). Among the 4000 PAH spectra in PAHdb, we chose 288 for the fitting based on the following criteria: 1) the molecules contain C, H, and N atoms only; 2) the molecules include aromatic C-H bonds that are responsible for UIE; (3) the numbers of selected small-, medium-, and large-sized PAHs (with carbon-atom number < 50, 50–100, and > 100) should be roughly the same to avoid a bias toward the PAHs with a specific size; 4) for each selected PAH, the spectrum of its cation should be available. The molecular formula and UID of the selected PAHs are presented in Supplementary Appendix S1 of the Supplementary Material. Following previous studies (Rosenberg et al., 2014; Zhang and Kwok, 2015), we performed a line broadening by convoluting with a Gaussian profile of a width of 15 cm^{-1}. Using the online tools provided by PAHdb, the normalized fitting spectra were finally deduced under an assumption of thermal excitation with temperatures ranging from 100 to 150 K.

1 www.astrochemistry.org/pahdb/

TABLE 1 χ^2_{red} of the fits.

Source	Temperature (*K*)	χ^2_{red} (PAH)	χ^2_{red} (fullerane)
IRAS 06530–0213	100	6.35	0.407
	125	2.69	0.298
	150	2.89	0.263
IRAS 05341 + 0852	100	0.753	0.0836
	125	0.361	0.0851
	150	1.91	0.0880
IRAS 07430 + 1115	100	1.15	0.236
	125	0.272	0.244
	150	0.293	0.249
IRAS 05113 + 1347	100	0.377	0.125
	125	0.242	0.221
	150	0.401	0.262
IRAS 19477 + 2401	100	1.35	0.0621
	125	0.840	0.105
	150	3.92	0.502
IRAS 04296 + 3429	100	0.255	0.280
	125	0.297	0.260
	150	0.394	0.326
IRAS 22223 + 4327	100	0.187	0.0893
	125	0.104	0.114
	150	0.229	0.140
IRAS 23304 + 6147	100	4.48	0.758
	125	3.54	0.758
	150	3.92	0.835
IRAS 22574 + 6609	100	1.72	0.121
	125	0.697	0.133
	150	0.283	0.142

2.3 Theoretical spectra of fulleranes

Theoretically calculated IR spectra of 55 fulleranes ($C_{60}H_m$, m = 2, 4, 6, 8, 10, 12, 14, 16, 18, 20, and 36) were taken from our previous works (Zhang et al., 2017).Two DFT hybrid functionals B3LYP and BH&HLYP in combination with PC1 basis set (Jensen, 2001; 2002) have been applied to the computations. Gaussian09 quantum chemistry package (Frisch, 2009) was used for this purpose. Five structural isomers have been considered for each $C_{60}H_m$ fulleranes. Fulleranes with an odd number of hydrogen atoms are thermodynamically less favorable than those with an even number and thus were not considered in this study (Kabo et al., 2010). The line broadening was performed by convoluting a Gaussian profile with a width of 15 cm^{-1}. To simulate the thermal excitation model, we multiplied the theoretical spectra by a temperature-dependent Planck function. All of the assumptions for constructing fullerane spectra are the same as those for PAH spectra, minimizing potential biases in comparison of their fitting results.

2.4 Spectra fitting

The nine continuum-subtracted spectra were fitted by synthesizing separately the theoretical spectra of PAHs and those of fulleranes using the Markov chain Monte Carlo algorithm. The steps involved were as follows.

1. Import the observational spectrum and the spectrum data matrix of PAHs/fulleranes.
2. Generate a series of random numerical sequences, each containing the same number of digits as the number of molecules in the spectrum data matrix.
3. Multiplying the spectrum data matrix with the numerical sequence, we get a series of synthesized spectra.
4. Compare the observed spectrum and the synthesized spectra, and pick up that with the minimum error.
5. Repeat the above steps until no synthesized spectrum with lower error can be found.
6. Output the synthesized spectrum and the numerical sequence given by the optimal fitting.

The goodness of the fits is evaluated quantitatively by the reduced chi-square (χ^2_{red}), with a smaller χ^2_{red} indicating a better fit. The calculations of χ^2_{red} were mainly based on the spectra within the wavelength range from 17.4 to 23.4 μm. However, multiple spectral features could be seen outside this wavelength coverage, which might originate from different species. At these wavelength ranges ($< 7.4\ \mu$m and $> 23.4\ \mu$m), the errors were accounted in the χ^2_{red} calculations only when the synthesized spectrum was more intense than the observed one.

After the optimal fitting was obtained, we can investigate the types of PAHs and fulleranes that are mostly responsible for the 21 μm feature. For that purpose, the PAHs were classified according to their sizes, charge states, number of nitrogen atoms, and C/H ratios; the fulleranes were classified according to their hydrogenation degrees.

3 Result and discussion

As thermal excitation has been assumed, the synthesized spectra depend on the preset temperatures. If the preset temperature was too high, in the short-wavelength regions, the synthesized spectra would exhibit too intense features to be compatible with the observations, and *vice versa*. To optimize the temperature adopted, we performed the fitting using a few different temperature values for PAH and

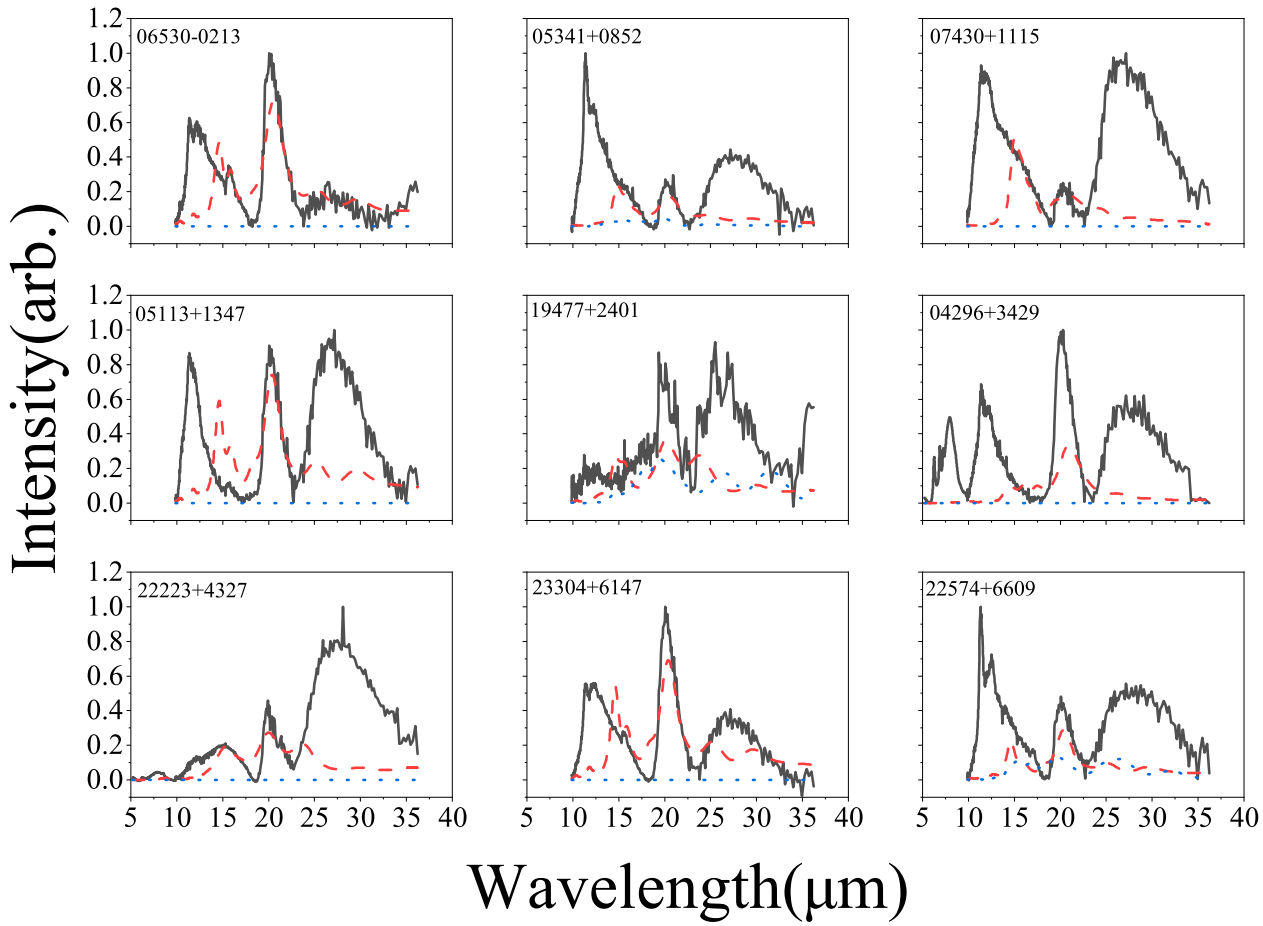

FIGURE 4
Contributions of the fulleranes with different hydrogenation to the fits. The solid curves show the observed spectra. The blue dotted and red dashed curves represent the spectra of $C_{60}H_m$ with $m \leq 10$ and $m > 10$, respectively.

fullerane spectra, as shown in Figures 2, 3 respectively. As shown in the figures, when the preset temperature is 150 K, the synthesized spectra show too strong emission bands near 12.7 μm. When it is 100 K, the band around 30 μm appears to be too intense. Therefore, we adopted a temperature of 125 K for the fitting.

The χ^2_{red} values of the fits are listed in Table 1. It is shown that adopting a temperature of 125 K gives the optimal choice for the PAH spectral fitting. Notably, χ^2_{red}(fullerane) are generally much smaller than χ^2_{red}(PAH), suggesting that fulleranes are more plausible to reproduce the 21 μm feature than PAHs. Therefore, in the following, we will focus on the discussion of the fitting results of fulleranes. For the PAH spectral fitting, the contributions from different PAH groups are illustrated by Supplementary Appendix S2 in the Supplementary Material.

The fulleranes are divided into two groups according to their hydrogenation degree ($C_{60}H_m$ with $m \leq 10$ and $m > 10$). Figure 4 shows the contributions of the two groups to the best fits (Figure 3). It is clear that slightly hydrogenated C_{60} cannot contribute to the emission band around 21 μm, which are mostly from the fulleranes with moderate hydrogen content (m = 10–36). This supports the finding of Zhang (2020) that moderately hydrogenated C_{60} are a promising carrier material producing the 21 μm feature, and is consistent with the experimental results (Cataldo, 2003; Iglesias-Groth et al., 2012).

C_{60} can be formed in the PPN phase (Zhang and Kwok, 2011). However, it seems that the C_{60} and 21 μm PPNe are mutually exclusive. No 21 μm source exhibits the C_{60} bands. The C_{60} PPN has a hotter central star than the 21 μm PPNe, and thus is more evolved (Zhang et al., 2010). The deep spectroscopy of two PNe exhibiting strong C_{60} bands do not detect the C-H stretching bands of fulleranes around 3.4–3.6 μm (Díaz-Luis et al., 2016). Theoretically, The emission bands from carbon-cage vibrations are still visible for slightly hydrogenated C_{60}, and gradually fade with increasing hydrogenation (Zhang et al., 2017). Consequently, a reasonable hypothesis is that the moderately hydrogenated C_{60} responsible for the 21 μm the feature could be formed in the early PPN stage, and then, with further increasing temperature of the central, is rapidly dehydrogenated by the intense ultraviolet radiation. In the PN stage, hydrogen atoms are completely removed from C_{60} surface so that no C-H band could be observed.

The binding energy of hydrogen atoms linking on fullerene surface is 3.3 eV and 1.9 eV for fulleranes with even and odd hydrogen-atom numbers, respectively (Abbink et al., 2024). The values are lower than that of ordinary H-H bonds (~4.5 eV). Therefore, C_{60} cannot be effectively hydrogenated if hydrogen is mainly in molecular state. Glassgold and Huggins (1983) found

that the ejected hydrogen from an AGB star remains in molecular state until the stellar temperature exceeds 2500 K. Therefore, atomic hydrogen dominates the stellar wind when the AGB envelope enter the PPN stage, and efficiently hydrogenates fullerenes. As a result of the dramatic changes of the physical conditions of PPNe, fulleranes are rapidly formed and then are rapidly dehydrogenated. If fullerenes are heavily hydrogenated, the carbon cage is unstable, and may be destructed. These can explain the transient nature of the 21 μm feature.

The C-H streching vibration of moderately hydrogenated fullerenes may provide observable emission features around 3.4 μm (Iglesias-Groth et al., 2012). Unfortunately, this feature lies outside the wavelength coverage of *Spitzer* spectra. Previous observations have revealed that the 21 μm sources are enriched with aliphatic features (Kwok et al., 2001), which may partly origin from fulleranes. It is highly desirable to investigate the correlation between the intensities of the 3.4 μm and 21 μm features. The James Webb Space Telescope could add light on this topic.

4 Conclusion

To examine the possibility of PAHs and fulleranes as the carrier of the 21 μm emission feature, we fit the infrared spectra of nine PNe exhibiting the 21 μm feature. The result shows that fulleranes can provide a better match than PAHs. Further analysis suggests that if fulleranes are responsible for the 21 μm feature, their hydrogenation degree must be moderate. The intense mass loss and rapidly increasing ultraviolet radiation of PPNe provide favorable environments for the formation of moderately hydrogenated fullerenes. During further evolution, fulleranes are readily dehydrogenated or destructed, providing a plausible interpretation for the rarity of the 21 μm feature.

Nevertheless, we have no means to draw firm conclusions at this moment. We hope that this work could attract research interests in fulleranes in space as collaborative efforts in observations, theories, and experiments are required.

Data availability statement

The original contributions presented in the study are included in the article/Supplementary Material, further inquiries can be directed to the corresponding author.

Author contributions

X-XL: Writing–original draft, Writing–review and editing, Investigation, Formal Analysis, Software, Visualization. YZ: Investigation, Writing–original draft, Writing–review and editing, Conceptualization, Data curation, Funding acquisition, Methodology, Project administration, Resources, Supervision, Validation. SS: Data curation, Formal Analysis, Validation, Writing–original draft, Writing–review and editing.

Funding

The author(s) declare that financial support was received for the research, authorship, and/or publication of this article. The authors declare that financial support was received for the research, authorship, and/or publication of this article. The financial supports of this work are from the National Natural Science Foundation of China (NSFC, No. 12473027, 12473027, and 12333005), the Guangdong Basic and Applied Basic Research Funding (No. 2024A1515010798), and the science research grants from the China Manned Space Project (NO. CMS-CSST-2021-A09, CMS-CSST-2021-A10, etc.). This article is based upon work from COST Action CA21126 - Carbon molecular nanostructures in space (NanoSpace), supported by COST (European Cooperation in Science and Technology).

Acknowledgments

The NASA Ames PAH IR Spectroscopic Database is gratefully acknowledged.

Conflict of interest

The authors declare that the research was conducted in the absence of any commercial or financial relationships that could be construed as a potential conflict of interest.

Publisher's note

Supplementary Material

The Supplementary Material for this article can be found online at: https://www.frontiersin.org/articles/10.3389/fspas.2024.1489982/full#supplementary-material

References

Abbink, D., Foing, B., and Ehrenfreund, P. (2024). A model for the hydrogenation and charge states of fullerene C_{60}: implications for diffuse interstellar band research. *Astronomy and Astrophysics* 684, A165–A175. doi:10.1051/0004-6361/202347478

Bauschlicher, C. W., Boersma, C., Ricca, A., Mattioda, A. L., Cami, J., Peeters, E., et al. (2010). The NASA Ames polycyclic aromatic hydrocarbon infrared spectroscopic database: the computed spectra. *Astrophysical J. Suppl. Ser.* 189 (2), 341–351. doi:10.1088/0067-0049/189/2/341

Bauschlicher, C. W., Ricca, A., Boersma, C., and Allamandola, L. J. (2018). The NASA Ames PAH IR spectroscopic database: computational version 3.00 with updated content and the introduction of multiple scaling factors. *Astrophysical J. Suppl. Ser.* 234 (2), 32–41. doi:10.3847/1538-4365/aaa019

Buss Jr, R. H., Cohen, M., Tielens, A. G. G. M., Werner, M. W., Bregman, J. D., Witteborn, F. C., et al. (1990). Hydrocarbon emission features in the IR spectra of warm supergiants. *Astrophysical J.* 365, L23–L26. doi:10.1086/185879

Cami, J., Bernard-Salas, J., Peeters, E., and Malek, S. E. (2010). Detection of C_{60} and C_{70} in a young planetary nebula. *Science* 329 (5996), 1180–1182. doi:10.1126/science.1192035

Cataldo, F. (2003). Fullerane, the hydrogenated C_{60}Fullerene: properties and astrochemical considerations. *Fullerenes, Nanotub. Carbon Nanostructures* 11 (4), 295–316. doi:10.1081/FST-120025852

Cataldo, F., and Iglesias-Groth, S. (2009). On the action of UV photons on hydrogenated fulleranes $C_{60}H_{36}$and $C_{60}D_{36}$. *Mon. Notices R. Astronomical Soc.* 400 (1), 291–298. doi:10.1111/j.1365-2966.2009.15457.x

Cerrigone, L., Hora, J. L., Umana, G., Trigilio, C., Hart, A., and Fazio, G. (2011). Identification of three new protoplanetary nebulae exhibiting the unidentified feature at 21 m. *Astrophysical J.* 738 (2), 121–129. doi:10.1088/0004-637X/738/2/121

Díaz-Luis, J. J., García-Hernández, D. A., Manchado, A., and Cataldo, F. (2016). A search for hydrogenated fullerenes in fullerene-containing planetary nebulae. *Astronomy Astrophysics* 589, 5–11. doi:10.1051/0004-6361/201527727

Duley, W. W., and Williams, D. A. (1981). The infrared spectrum of interstellar dust: surface functional groups on carbon. *Mon. Notices R. Astronomical Soc.* 196 (2), 269–274. doi:10.1093/mnras/196.2.269

Evans, A., van Loon, J. T., Woodward, C. E., Gehrz, R. D., Clayton, G. C., Helton, L. A., et al. (2012). Solid-phase in the peculiar binary XX Oph? *Mon. Notices R. Astronomical Soc. Lett.* 421 (1), L92–L96. doi:10.1111/j.1745-3933.2012.01213.x

Frisch, M. J. E. A. (2009). *Gaussian 09, Revision d. 01, Gaussian*. Wallingford CT: Inc, 201.

García-Hernández, D. A., Iglesias-Groth, S., Acosta-Pulido, J. A., Manchado, A., García-Lario, P., Stanghellini, L., et al. (2011a). The formation of fullerenes: clues from new c_{60}, c_{70}, and (possible) planar c_{24} detections in magellanic cloud planetary nebulae. *Astrophysical J. Lett.* 737 (2), L30–L37. doi:10.1088/2041-8205/737/2/L30

García-Hernández, D. A., Manchado, A., García-Lario, P., Stanghellini, L., Villaver, E., Shaw, R. A., et al. (2010). Formation of fullerenes in H-containing planetary nebulae. *Astrophysical J. Lett.* 724 (1), L39–L43. doi:10.1088/2041-8205/724/1/L39

García-Hernández, D. A., Rao, N. K., and Lambert, D. L. (2011b). Are C molecules detectable in circumstellar shells of R Coronae Borealis stars? *Astrophysical J.* 729 (2), 126–131. doi:10.1088/0004-637X/729/2/126

García-Lario, P., Manchado, A., Ulla, A., and Manteiga, M. (1999). Infrared space observatory observations of IRAS 16594–4656: a new Proto-planetary nebula with a strong 21 micron dust feature. *Astrophysical J.* 513 (2), 941–946. doi:10.1086/306895

Gehrz, R. D., Roellig, T. L., Werner, M. W., Fazio, G. G., Houck, J. R., Low, F. J., et al. (2007). The NASA Spitzer space telescope. *Rev. Sci. Instrum.* 78 (1), 011302. doi:10.1063/1.2431313

Gielen, C., Cami, J., Bouwman, J., Peeters, E., and Min, M. (2011). Carbonaceous molecules in the oxygen-rich circumstellar environment of binary post-AGB stars: C_{60}fullerenes and polycyclic aromatic hydrocarbons. *Astronomy and Astrophysics* 536, A54–A62. doi:10.1051/0004-6361/201117961

Gładkowski, M., Szczerba, R., Sloan, G. C., Lagadec, E., and Volk, K. (2019). 30-micron sources in galaxies with different metallicities. *Astronomy and Astrophysics* 626, A92–A126. doi:10.1051/0004-6361/201833920

Glassgold, A. E., and Huggins, P. J. (1983). Atomic and molecular hydrogen in the circumstellar envelopes of late-type stars. *Mon. Notices R. Astronomical Soc.* 203, 517–532. doi:10.1093/mnras/203.2.517

Hrivnak, B. J., Volk, K., and Kwok, S. (2000). 2-45 micron infrared spectroscopy of carbon-rich proto-planetary nebulae. *Astrophysical J.* 535 (1), 275–292. doi:10.1086/308823

Hrivnak, B. J., Volk, K., and Kwok, S. (2009). A Spitzer study of 21 and 30m emission in several galactic carbon-rich protoplanetary nebulae. *Astrophysical J.* 694 (2), 1147–1160. doi:10.1088/0004-637X/694/2/1147

Iglesias-Groth, S., García-Hernández, D. A., Cataldo, F., and Manchado, A. (2012). Infrared spectroscopy of hydrogenated fullerenes (fulleranes) at extreme temperatures. *Mon. Notices R. Astronomical Soc.* 423 (3), 2868–2878. doi:10.1111/j.1365-2966.2012.21097.x

Jensen, F. (2001). Polarization consistent basis sets: principles. *J. Chem. Phys.* 115 (20), 9113–9125. doi:10.1063/1.1413524

Jensen, F. (2002). Polarization consistent basis sets. II. Estimating the Kohn–Sham basis set limit. *J. Chem. Phys.* 116 (17), 7372–7379. doi:10.1063/1.1465405

Kabo, G. J., Karpushenkava, L. S., and Paulechka, Y. U. (2010). "Thermodynamic properties of fullerene hydrides C and equilibria," in *Fullerane: the hydrogenated fullerenes*. Editors F. Cataldo, and S. Iglesias-Groth, 55–83.

Kwok, S., (1993). Proto-planetary nebulae. In *Symp. - int. Astron. Union, symposium-international astronomical union*. 155, 263–270. doi:10.1017/s0074180900170998Cambridge University Press

Kwok, S. (2004). The synthesis of organic and inorganic compounds in evolved stars. *Nature* 430 (7003), 985–991. doi:10.1038/nature02862

Kwok, S. (2024). Planetary nebulae research: past, present, and future. *Galaxies* 12 (4), 39–57. doi:10.3390/galaxies12040039

Kwok, S., Volk, K., and Bernath, P. (2001). On the origin of infrared plateau features in proto-planetary nebulae. *Astrophysical J.* 554 (1), L87–L90. doi:10.1086/320913

Kwok, S., Volk, K. M., and Hrivnak, B. J. (1989). A 21 micron emission feature in four proto-planetary nebulae. *Astrophysical J.* 345 (Oct. 1), L51–L54. doi:10.1086/185550

Li, A., Liu, J. M., and Jiang, B. W. (2013). On iron monoxide nanoparticles as a carrier of the mysterious 21 m emission feature in post-asymptotic giant branch stars. *Astrophysical J.* 777 (2), 111–117. doi:10.1088/0004-637X/777/2/111

Matsuura, M., Bernard-Salas, J., Lloyd Evans, T., Volk, K. M., Hrivnak, B. J., Sloan, G. C., et al. (2014). Spitzer Space Telescope spectra of post-AGB stars in the Large Magellanic Cloud–polycyclic aromatic hydrocarbons at low metallicities. *Mon. Notices R. Astronomical Soc.* 439 (2), 1472–1493. doi:10.1093/mnras/stt2495

Mattioda, A. L., Hudgins, D. M., Boersma, C., Bauschlicher, C. W., Ricca, A., Cami, J., et al. (2020). The NASA Ames PAH IR spectroscopic database: the laboratory spectra. *Astrophysical J. Suppl. Ser.* 251 (2), 22–37. doi:10.3847/1538-4365/abc2c8

Neugebauer, G., Habing, H. J., Van Duinen, R., Aumann, H. H., Baud, B., Beichman, C. A., et al. (1984). The infrared astronomical satellite (IRAS) mission. *Astrophysical J.* 278 (March 1), L1–L6. doi:10.1086/184209

Otsuka, M., Kemper, F., Hyung, S., Sargent, B. A., Meixner, M., Tajitsu, A., et al. (2013). The detection of C in the well-characterized planetary nebula M1-11. *Astrophysical J.* 764 (1), 77–96. doi:10.1088/0004-637X/764/1/77

Palotás, J., Martens, J., Berden, G., and Oomens, J. (2020). The infrared spectrum of protonated buckminsterfullerene C60H+. *Nat. Astron.* 4 (3), 240–245. doi:10.1038/s41550-019-0941-6

Papoular, R. (2011). Candidate carriers and synthetic spectra of the 21- and 30m proto-planetary nebular bands. *Mon. Notices R. Astronomical Soc.* 415, 494–502. doi:10.1111/j.1365-2966.2011.18724.x

Parr, R. G. (1985). "Density functional theory in Chemistry," in *Density functional methods in physics* (Boston, MA: Springer US), 141–158.

Roberts, K. R., Smith, K. T., and Sarre, P. J. (2012). Detection of C60 in embedded young stellar objects, a Herbig Ae/Be star and an unusual post-asymptotic giant branch star: C60 in young stellar and other objects. *Mon. Notices R. Astronomical Soc.* 421 (4), 3277–3285. doi:10.1111/j.1365-2966.2012.20552.x

Rosenberg, M. J. F., Berné, O., and Boersma, C. (2014). Random mixtures of polycyclic aromatic hydrocarbon spectra match interstellar infrared emission. *Astronomy Astrophysics* 566, L4–L10. doi:10.1051/0004-6361/201423953

Rüchardt, C., Gerst, M., Ebenhoch, J., Campbell, E. E., Tellgmann, R., Schwarz, H., et al. (1993). Transfer hydrogenation and deuteration of buckminsterfullerene C_{60} by 9,10-dihydroanthracene and 9,9′,10,10′[D_4]Dihydroanthracene. *Angew. Chemie-International Ed.* 32 (4), 584–586. doi:10.1002/anie.199305841

Sadjadi, S. A., and Parker, Q. A. (2021). It remains a cage: ionization tolerance of C_{60} fullerene in planetary nebulae. *FNCN* 29, 620–625. doi:10.1080/1536383x.2021.1876677

Sellgren, K., Werner, M. W., Ingalls, J. G., Smith, J. D. T., Carleton, T. M., and Joblin, C. (2010). C_{60} IN REFLECTION NEBULAE. *Astrophysical J. Lett.* 722 (1), L54–L57. doi:10.1088/2041-8205/722/1/L54

Tielens, A. G. G. M. (2008). Interstellar polycyclic aromatic hydrocarbon molecules. *Annu. Rev. Astronomy Astrophysics* 46, 289–337. doi:10.1146/annurev.astro.46.060407.145211

Van Winckel, H. (2003). Post-AGB stars. *Annu. Rev. Astronomy Astrophysics* 41 (1), 391–427. doi:10.1146/annurev.astro.41.071601.170018

Volk, K., Hrivnak, B. J., Matsuura, M., Bernard-Salas, J., Szczerba, R., Sloan, G. C., et al. (2011). Discovery and analysis of 21 m feature sources in the magellanic clouds. *Astrophysical J.* 735 (2), 127–154. doi:10.1088/0004-637X/735/2/127

Volk, K., Sloan, G. C., and Kraemer, K. E. (2020). The 21 m and 30 m emission features in carbon-rich objects. *Astrophysics Space Sci.* 365, 88–25. doi:10.1007/s10509-020-03798-2

Volk, K. M., and Kwok, S. (1989). Evolution of protoplanetary nebulae. *Astrophysical J.* 342 (July 1), 345–363. doi:10.1086/167597

Webster, A. (1995). The lowest of the strongly infrared-active vibrations of the fulleranes and astronomical emission band at a wavelength of 21m. *Mon. Notices R. Astronomical Soc.* 277 (4), 1555–1566. doi:10.1093/mnras/277.4.1555

Zhang, K., Jiang, B. W., and Li, A. (2009). On the carriers of the 21m emission feature in post-asymptotic giant branch stars. *Mon. Notices R. Astronomical Soc.* 396, 1247–1256. doi:10.1111/j.1365-2966.2009.14808.x

Zhang, Y. (2020). Are fulleranes responsible for the 21 micron feature? *Chin. J. Chem. Phys.* 33, 101–106. doi:10.1063/1674-0068/cjcp1911203

Zhang, Y., and Kwok, S. (2011). DETECTION OF C_{60}IN THE PROTOPLANETARY NEBULA IRAS 01005+7910. *Astrophysical J.* 730 (2), 126–130. doi:10.1088/0004-637X/730/2/126

Zhang, Y., and Kwok, S. (2015). On the viability of the PAH model as an explanation of the unidentified infrared emission features. *Astrophysical J.* 798 (1), 37–42. doi:10.1088/0004-637X/798/1/37

Zhang, Y., Kwok, S., and Hrivnak, B. J. (2010). A spitzer/infrared spectrograph spectral study of a sample of galactic carbon-rich proto-planetary nebulae. *Astrophysical J.* 725 (1), 990–1001. doi:10.1088/0004-637X/725/1/990

Zhang, Y., Sadjadi, S., and Hsia, C. H. (2020). Hydrogenated fullerenes (fulleranes) in space. *Astrophysics Space Sci.* 365 (4), 67–74. doi:10.1007/s10509-020-03779-5

Zhang, Y., Sadjadi, S., Hsia, C. H., and Kwok, S. (2017). Search for hydrogenated C_{60} (fulleranes) in circumstellar envelopes. *Astrophysical J.* 845 (1), 76–91. doi:10.3847/1538-4357/aa71ac